Computer Modeling in Engineering & Sciences

Tech Science Press

https://doi.org/10.32604/cmes.2026.081075

ARTICLE

Fractional Order *In Vitro* Fertilization Model Real Data Analysis with Novel Application of Inequalities via Stability and Computational Techniques

Manal Ghannam[1], Bilgen Kaymakamzade[1,2], Muhammad Farman[1,3,4], Kottakkaran Sooppy Nisar[5,*] and Mohammed Altaf Ahmed[6]

[1]Department of Mathematics, Mathematical Research Center, Near East University, Mersin, Turkey
[2]Research Center of Applied Mathematics, Khazar University, Baku, Azerbaijan
[3]Faculty of Medicine, Department of Biostatistics and Medical Informatics, Karadeniz Technical University, Trabzon, Turkey
[4]International Center for Interdisciplinary Research in Sciences, The University of Lahore, Lahore, Pakistan
[5]Department of Mathematics, College of Science and Humanities, Prince Sattam bin Abdulaziz University, Al-Kharj, Saudi Arabia
[6]Department of Computer Engineering, College of Computer Engineering & Sciences, Prince Sattam Bin Abdulaziz University, Al-Kharj, Saudi Arabia

*Corresponding Author: Kottakkaran Sooppy Nisar. Email: n.sooppy@psau.edu.sa

Received: 23 February 2026; Accepted: 12 May 2026; Published: 27 July 2026

ABSTRACT: *In Vitro* Fertilization (IVF) has been a major medical advancement in the field of fertility treatment. It has helped millions of individuals and couples overcome infertility by providing a workable option. It involves removing eggs from the ovaries of a female, fertilizing those eggs with male sperm in a monitored lab condition. In this work, we developed a new model to show the success of *In Vitro* Fertilization rates in women through a fractional-order compartmental modeling framework by using real data. The developed model is analyzed statistically, and the biological feasibility of the model. The Lipschitz condition, expressed by the Lipschitz inequality, suggests that the change in a function's output is limited by a constant known as the Lipschitz constant in relation to the input changes between any two points in its domain. This characteristic ensures that solution routes remain consistent, resulting in well-behaved and singular solutions. The linear growth inequality describes the condition of linear growth by asserting that one variable can be limited by another that rises linearly. This inequality is crucial because it prevents differential equation solutions from rising too rapidly, ensuring that they remain within established boundaries. We used Volterra integral inequality with a Volterra-type Lyapunov function to analyze the fractional derivatives of Lyapunov functions in a fractional-order system, which is necessary to establish global asymptotic stability. This extends the standard Lyapunov stability theory to fractional-order systems, particularly in the analysis of complex models like the infectious disease model, by providing a method to constrain the behavior of the system without solving the differential equations explicitly. Additionally, a sensitivity analysis of several aspects is derived through mathematical simulations. Additionally, we use numerical simulations to validate our theoretical findings at different fractional orders.

KEYWORDS: *In vitro* fertilization; fertile oocyte donors; health care; volterra type inequality; lipschitz inequality; caputo operator

1 Introduction

Infertility is an issue that, unfortunately, many couples struggle with, up to 12 percent worldwide [1]. It is defined as a disease that causes the failure of conceiving after one year of unprotected sexual intercourse, according to the International Committee for Monitoring Assisted Reproductive Technology and the

World Health Organization [2]. *In Vitro* Fertilization (IVF) has been rapidly becoming a major Assisted Reproductive Technology (ART) to help couples facing such problems to achieve pregnancy [3–5]. The anniversary of the first "test-tube baby" birth was in 1978 on the 25th of July [6]. Different forms of infertility were addressed. These included female tubal disorders and/or inflammatory diseases, male spermatogenesis defects or insufficient sperm transport, couples experiencing long-term unexplained infertility, the presence of spermatozoa immunity in one or both spouses, and couples experiencing combined factors [7]. There are two different types of IVF cycles: regular IVF, where both the sperm and the oocyte are retrieved from the parents, and donor cycle IVF, where either the sperm or the oocyte (or both) was retrieved from a healthy, fertile donor [8]. Even so, concerns have been rising regarding the impact of factors like decreasing embryo implantation rates and increasing maternal age on IVF outcomes [9–11]. To have the first live birth following IVF and embryo transfer, there were certain challenges that had to be conquered, like ovarian stimulation, cycle monitoring, oocyte culture, sperm preparation and capacitation, etc. [12,13]. An important indicator of a successful embryo implantation after IVF is a positive beta-human chorionic gonadotropin (βHCG) [14,15].

Reproductive experts have struggled for years to predict the success of pregnancy in IVF cycles [16]. Using mathematical modeling to represent the IVF dynamics has become a very strong approach in medical research [17]. The two primary categories of mathematical models are empirical models and mechanistic models. Empirical models rely on data, which are frequently employed in medical research and are designed for prediction. Mechanistic models take into account the components of a system and how they interact. They excel in formulating, evaluating, and improving hypotheses [18].

An effective technique for analyzing an extensive diversity of real-life problems in many fields, in engineering and science, is applying the concept of a fractional calculus (FC), like Riemann-Liouville, Caputo, and Granöwald-Letnikov; all are among the theories that describe the derivative and integrated functions [19]. Since fractional calculus can model the majority of real-world problems, it has attracted a lot of attention in contemporary science and technology, in contrast to classical calculus. Numerous qualitative and numerical investigations of differential and integral equations of non-integer order have resulted from this [20–22].

Fractal-fractional operators are a new development in fractional calculus, which merge the characteristics of fractional power laws and fractal geometry to simulate even more complicated hereditary behavioral patterns [23]. This study uses the Caputo fractional derivative to preserve compatibility with the classical initial circumstances, while the fractal fractional operators show a good frontier for more improving reproductive models.

Due to its capacity to capture memory and hereditary effects that are not captured in traditional integer-order systems, fractional-order differential operators have garnered considerable interest in epidemiological modeling [24]. In biological and biomedical systems, fractional calculus has been effectively used to describe memory and inherited traits [25]. In spite of this, it has not been extensively used for predicting IVF outcomes. However, hormonal reactions, female ovarian reserve reduction, and embryo formation tracks are examples of biological procedures in reproductive health care that frequently display memory effects [26]. These impacts are not captured by typical integer order models.

This paper explores factors influencing positive βHCG rates, including the origin of oocytes (own vs. donor), embryo quality, and embryo status (fresh vs. frozen), and also evaluates the influence of the number of embryos transferred on the outcomes of the IVF cycles by analyzing the live birth rates associated with single vs. multiple embryo transfers. The main aim of this work is specifically to investigate these concerns at the Near East IVF Clinic in Northern Cyprus and, through the examination of these factors, to provide significant knowledge and understanding regarding the IVF procedures carried out at the Near East IVF

Clinic. The results will have a substantial impact on providing guidance to patients and shaping the creation of efficient public policies regarding ART. Using data from IVF clinics at Near East University Hospital that describe the factors that affect the success of pregnancy, such as the male and female factors. In contrast to simply statistical methods, this model takes into account the fundamental mechanics of IVF progress, and it uses a fractional order to detect memory effects. To validate the model, actual clinical data from Near East IVF Clinic are used to help in predicting the outcomes of IVF treatment, which is dependent on numerous factors. The findings of this study may provide significant and novel insights into the basic workings of the IVF process, enabling medical professionals to tailor therapies to each patient's specific needs and improve the chances of a successful pregnancy.

2 Materials and Methods

This paper employs a retrospective analysis of data from 253 IVF treatment cycles at Near East University Hospital between 2015 and 2023. Patient information, including male and female factors, donor details, and IVF outcomes, was obtained from clinical records approved by the Faculty of Medicine, Department of Medical Genetics, Near East University, Center of Excellence, and Mathematics Research Center. The study was conducted in accordance with relevant guidelines and regulations and received ethical approval under the number NEU/2024/121-1820. The data were anonymized, and participant identities could not be identified; therefore, informed consent was not required. The objective of the statistical analysis, conducted using IBM SPSS Statistics version 27 software, was to compare the rates of success among different groups of patients. A Chi-square test was conducted to examine the association between embryo quality categories (low, medium, high) and IVF success (positive βHCG outcome). This test determines whether embryo quality is significantly related to pregnancy outcomes. An independent samples t-test was used to compare the mean age between patients with successful IVF outcomes and those with unsuccessful outcomes, in order to assess the effect of maternal age on IVF success. A p-value is less than 0.05 was considered statistically significant.

Fig. 1 illustrates the stages that the regular IVF patients go through [27], starting with clinical and laboratory testing, setting up the IVF cycle, ordering drugs, signing paperwork, and obtaining nursing instruction, secondly, ovarian hyper stimulation from 8–12 days of drug injections to encourage the development of follicles, the source of future eggs, then, trigger injection when 3 or more dominant follicles at or over 17 mm are seen via ultrasound, to start oocyte pick-up (OPU) after 35–36 h by a quick, straightforward surgical operation carried out under anaesthesia, lasting 15 min. Now, if an oocyte is yielded in OPU, sperm is obtained, and fertilization of the oocytes via intracytoplasmic sperm injection (ICSI) technique is used, and the endometrium is supported with pure progesterone. The embryo is followed up for 2–5 days to continue its development. The last stage will be the embryo transfer, and after 12 days from the embryo transfer βHCG pregnancy test is done. The descriptive and the characteristics of the sample of the study are shown in Table 1. Different types of modalities were used in this data. Most embryo grading methods, such as the Istanbul Consensus, assign a grade of "good," (G1), "medium," (G2), or "poor" (G3) to embryos without employing a numerical index. The non-numerical factor-based criteria vary based on the architecture of the embryo evaluation system for each developmental stage. Therefore, using non-numerical indicators based on distinct evaluation standards makes it impossible to compare the features of groups of embryos at different developmental stages. Because of this, this type of comparison needs a numerical scoring system based on equivalent evaluation criteria [28]. From 2015 to 2023, about 253 patients of IVF treatment were included in this clinical data analysis. The data was obtained from the Near East University Hospital IVF clinic. This data, which consisted of patient files and clinical outcome records, is shown in Table 1. These are a select few variables and parameters that help highlight the factors that affect the result of IVF in Northern Cyprus.

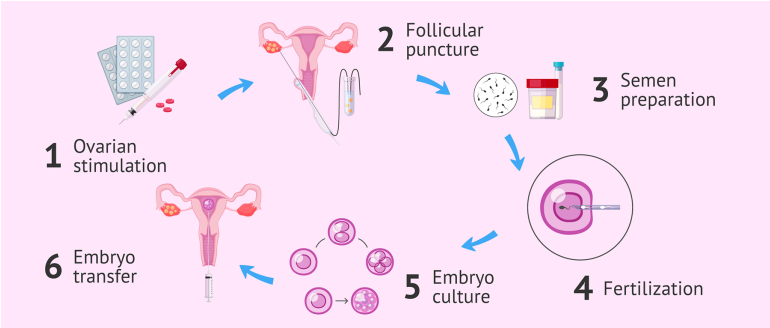

Figure 1: Schematic illustration of the general IVF stages.

Table 1: Characteristics and descriptive statistics of the data.

Clinical Data of the Sample	Regular IVF	Oocyte Donation
The average males age	42.30	40.58
The average females age	34.55	39.77
Fresh embryo positive βHCG rate	0.70	0.55
Frozen embryo positive βHCG rate	0.30	0.38
Frozen oocyte positive βHCG rate	–	0.06
The positive βHCG rate per single embryo transfer	0.09	0.02
The positive βHCG rate per double embryo transfer	0.40	0.32
The positive βHCG rate per triple embryo transfer	0.51	0.66
The positive βHCG rate associated with high-quality embryos	0.44	0.51
The positive βHCG rate associated with medium-quality embryos	0.35	0.34
The positive βHCG rate associated with poor-quality embryos	0.22	0.15

3 Formalization of Fractional Order IVF Model

It can be difficult to model IVF success because it involves many factors that affect the process itself. However, we can demonstrate this model with a particular example of a compartmental model using Caputo Fractional Calculus with six-compartment model of IVF, despite the fact that it won't cover every situation. The six compartments of the model are:

- $I(t)$: the number of infertile couples that diagnosed as Polycystic Ovary Syndrome (PCOS), male factors or female factors;
- $V(t)$: the number of patients under going IVF treatment including ovarian stimulation, egg retrieval, sperm collection and fertilization;
- $G_1(t)$: the number of high quality embryos;
- $G_2(t)$: the number of medium quality embryos;
- $G_3(t)$: the number of low quality embryos; and
- $F(t)$: the number of positive pregnancy results.

Here we consider some useful results of fractional calculus for model formulation and analysis for the given assumption.

Definition 1 ([25]): *Assume that* J *is a real value function on* $L^1([0,T],\mathbb{R})$ *so the Riemann Liouville fractional order* $\tau \in (0,1)$ *written as:*

$$ {}_0^{RL}D_t^{\tau}\mathrm{J}(t) = \frac{1}{\Gamma(\tau)}\int_0^t (t-\mu)^{(\tau-1)}\mathrm{J}(\mu)d\mu. \tag{1}$$

The interval $(0,\infty)$ *defines the integral on the right side.*

Definition 2 ([25]): *Let* J *be a real value function on* $[0,T]$. *then the Caputo derivative of* J *is:*

$$ {}_0^{C}D_t^{\tau}\mathrm{J}(t) = \frac{1}{\Gamma(n-\tau)}\left[\int_0^t (t-\mu)^{n-\mu-1}\frac{d^n}{d\mu^n}\mathrm{J}(t)(\mu)d\mu\right], \tag{2}$$

where the Gamma function is represented by the symbol $\Gamma(.)$

Let $n = 1$, *then the Eq. (2) can be expressed as:*

$$ {}_0^{C}D_t^{\tau}\mathrm{J}(t) = \frac{1}{\Gamma(n-\tau)}\left[\int_0^t (t-\mu)^{-\tau}\mathrm{J}'(t)(\mu)d\mu\right]. \tag{3}$$

Lemma 1: *Let* τ^* *be the Caputo systems equilibrium point, then*

$$ {}_0^{C}D_t^{\tau}\mathrm{J}(t) = \mathrm{J}(t,\tau(t)), \quad \tau \in (0,1), \tag{4}$$

if and only if $\mathrm{J}(t,\tau^*) = 0$.

Every interaction in the suggested compartmental model is directly connected to recognized clinical procedures in IVF treatment in order to improve biological interpretability. Transition from infertile couples to the second compartment represents the clinical decision and eligibility for IVF treatment. The associated rate reflects factors such as medical recommendation, patient choice, and access to fertility services, while the transitions from the compartment of IVF treatment to each of the embryo quality compartments are the result of fertilization, oocyte retrieval, ovarian stimulation, and embryo culture. Standard embryological grading systems based on morphological and developmental parameters are reflected in the distribution of embryos into low, medium, and high quality categories. The last transitions from embryo quality compartments to pregnancy outcome represent embryo transfer and implantation. The corresponding rates are interpreted as implantation probabilities, which are known to depend strongly on embryo quality, with high-quality embryos having significantly higher success rates.

A greater number of real systems are included in fractional-order systems, which are variations of conventional integer-order systems with a derivative between 0 and 1. We now extend and modify the model for examining IVF effectiveness using a set of fractional order equations inside the framework of the Caputo derivative, which is expressed as follows:

$$\begin{aligned}
&{}^{C}D_t^{\tau}I(t) = \pi N - \mu_1 I - \beta I,\\
&{}^{C}D_t^{\tau}V(t) = \beta I - (\mu_2 + \alpha_1 + \alpha_2 + \alpha_3)V,\\
&{}^{C}D_t^{\tau}G_1(t) = \alpha_1 V - (\gamma_1 + \mu)G_1,\\
&{}^{C}D_t^{\tau}G_2(t) = \alpha_2 V - (\gamma_2 + \mu)G_2,\\
&{}^{C}D_t^{\tau}G_3(t) = \alpha_3 V - (\gamma_3 + \mu)G_3,\\
&{}^{C}D_t^{\tau}F(t) = (\gamma_1 G_1 + \gamma_2 G_2 + \gamma_3 G_3)\frac{1}{1+\sigma E} - \mu F.
\end{aligned} \tag{5}$$

The fractional-order IVF model is built using the following assumptions to guarantee biological explanation and mathematical simplicity:

1. The initial conditions are:

$$I(0) = I_0 \geq 0, \quad V(0) = 0 \geq 0, \quad G_1(0) = 0 \geq 0, \quad G_2(0) = 0 \geq 0, \quad G_3(0) = 0 \geq 0, \quad F(0) = 0 \geq 0. \tag{6}$$

2. People move through the compartments only in one direction.

3. Embryos are classified into groups of poor, medium, and high quality. There is a unique and consistent implantation probability for every class.

4. The chance of obtaining a positive βHCG result is influenced separately by every embryo's quality group.

5. A decreasing function that is added into the transition rates to the pregnancy compartment is used to describe how the chance of an effective implantation declines with maternal age.

6. A positive βHCG test, is the definition of IVF success which indicates biochemical pregnancy and does not model future phases like live birth.

7. All of the parameters are assumed to be constant and positive.

The dynamical system is depicted in Fig. 2, while Table 2 provides a description of each parameter.

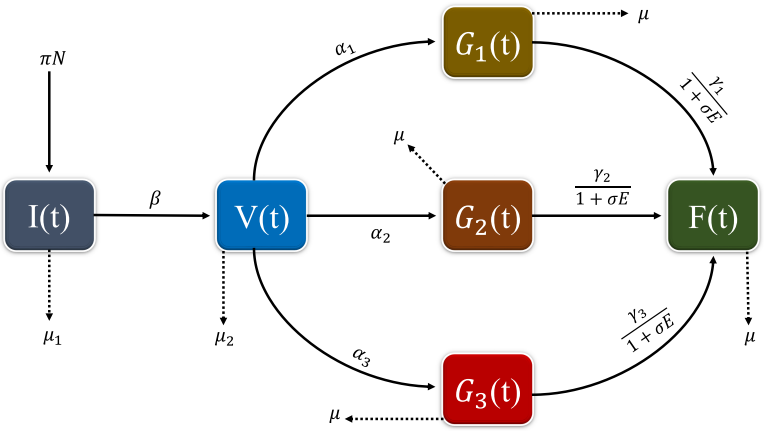

Figure 2: Flow chart of dynamical system.

Table 2: The parameters description.

Symbol	Explanation
π	The rate of infected patients that assumed to be new infertile couples enter the system
μ_1	The rate of recovery from infertility after normal medication or leaving without IVF
μ_2	The rate of IVF early failure due to female or male factors
β	The rate of IVF treatment when infertile couples starting IVF procedure
α_1	The rate of embryos formation with high quality during IVF
α_2	The rate of embryos formation with medium quality during IVF
α_3	The rate of embryos formation with low quality during IVF
γ_1	The rate of the high quality embryos implantation success

(Continued)

Table 2 (continued)

Symbol	Explanation
γ_2	The rate of the medium quality embryos implantation success
γ_3	The rate of the low quality embryos implantation success
σ	The rate of female age effect on implantation
E	Female average age
N	Total Population of infertile couples
μ	Rate of wasting the embryo after biochemical pregnancy.

Where, γ_1 represents the probability that an embryo of high quality produces a positive pregnancy, γ_2 is the probability that an embryo of medium quality produces a positive pregnancy, and γ_3 is the probability that an embryo of low quality produces a positive pregnancy.

All metrics, including embryo grading distributions, implantation rates, and treatment results, are specified in biologically meaningful ways and correlate to quantifiable clinical quantities that have been taken from an IVF clinic. The model equations' dimensional consistency is maintained by the appropriate selection of units. Noted that the Parameters are estimated using empirical proportions from clinical data and refined through curve fitting to match observed IVF outcomes.

4 Analysis of the Model

4.1 Equilibrium Point Analysis

The equilibrium points will be checked in this section. As the system (5) is a flow system but not infectious one, then equilibrium points are:

$$\mathbb{E}^* = \left(I^*, V^*, G_1^*, G_2^*, G_3^*, F^*\right),$$

where

$$I^* = \frac{\pi N}{\mu_1 + \beta}, \quad V^* = \frac{\beta \pi N}{(\mu_1 + \beta)(\mu_2 + \alpha_1 + \alpha_2 + \alpha_3)}, \quad G_1^* = \frac{\alpha_1 \beta \pi N}{(\gamma_1 + \mu)(\mu_1 + \beta)(\mu_2 + \alpha_1 + \alpha_2 + \alpha_3)},$$
$$G_2^* = \frac{\alpha_2 \beta \pi N}{(\gamma_2 + \mu)(\mu_1 + \beta)(\mu_2 + \alpha_1 + \alpha_2 + \alpha_3)}, \quad G_3^* = \frac{\alpha_3 \beta \pi N}{(\gamma_3 + \mu)(\mu_1 + \beta)(\mu_2 + \alpha_1 + \alpha_2 + \alpha_3)}. \tag{7}$$

The suggested system is considered absolutely stable. At this equilibrium point, stability means a constant flow of infertile couples, constant treatment rate with a stable embryo distribution and success rate [29], which leads to a clinical steady state.

4.2 The Reproduction Number (IVF Success Threshold)

In disease epidemiology, the basic reproduction number is a threshold quantity that establishes whether or not a disease can be controlled. When calculating this number for biological models, researchers frequently employ the next-generation matrix technique [30]. As this model is not a model of infectious disease, a definition of IVF success threshold is defined using [31,32], to be:

$\mathbf{R}_s$ = total successful implantation rate/loss rate

then,

$$\mathbf{R}_s = \frac{\alpha_1\gamma_1 + \alpha_2\gamma_2 + \alpha_3\gamma_3}{\mu(1+\sigma E)}. \tag{8}$$

The $\mathbf{R}_0$ which is the basic reproduction number, indicates how likely it is for a disease to spread throughout a community. It is mathematically associated with the peak and ultimate extent of an epidemic and serves as a threshold for the stability of a disease-free equilibrium. In the suggested model, the IVF success threshold $\mathbf{R}_s$ will be used instead, which can be defined as the typical quantity of viable embryos produced, under optimal circumstances.

4.3 Sensitivity Analysis

Definition 3 ([31]): *Sensitivity analysis is a mathematical technique used to quantify how variations in model parameters affect the behavior of the system.*

For a fractional-order dynamical system, the sensitivity of a state variable $y(t)$ with respect to a parameter r is defined as:

$$S_r(t) = \frac{\partial y(t)}{\partial r}.$$

In normalized form, the sensitivity function is given by:

$$S_r^{rel}(t) = \frac{r}{y(t)} \cdot \frac{\partial y(t)}{\partial r}.$$

This measure describes the relative change in the state variable due to a relative change in the parameter. In the context of fractional-order models, sensitivity analysis is particularly important due to the presence of memory effects, where parameter variations may influence the system dynamics over time.

The impact of each parameter in $\mathbf{R}_s$ is demonstrated by the analytical examples that follow:

$$\begin{aligned}
&\sum_{\mu}^{\mathbf{R}_s} = -1 < 0, \quad \sum_{\sigma}^{\mathbf{R}_s} = -\frac{\sigma E}{(1+\sigma E} < 0,\\
&\sum_{\alpha_1}^{\mathbf{R}_s} = \frac{\alpha_1\gamma_1}{(\alpha_1\gamma_1 + \alpha_2\gamma_2 + \alpha_3\gamma_3)} > 0\\
&\sum_{\alpha_2}^{\mathbf{R}_s} = \frac{\alpha_2\gamma_2}{(\alpha_1\gamma_1 + \alpha_2\gamma_2 + \alpha_3\gamma_3)} > 0\\
&\sum_{\alpha_3}^{\mathbf{R}_s} = \frac{\alpha_3\gamma_3}{(\alpha_1\gamma_1 + \alpha_2\gamma_2 + \alpha_3\gamma_3)} > 0\\
&\sum_{\gamma_1}^{\mathbf{R}_s} = \frac{\alpha_1\gamma_1}{(\alpha_1\gamma_1 + \alpha_2\gamma_2 + \alpha_3\gamma_3)} > 0\\
&\sum_{\gamma_2}^{\mathbf{R}_s} = \frac{\alpha_2\gamma_2}{(\alpha_1\gamma_1 + \alpha_2\gamma_2 + \alpha_3\gamma_3)} > 0\\
&\sum_{\gamma_3}^{\mathbf{R}_s} = \frac{\alpha_3\gamma_3}{(\alpha_1\gamma_1 + \alpha_2\gamma_2 + \alpha_3\gamma_3)} > 0.
\end{aligned} \tag{9}$$

A positive sensitivity index indicates that as the related parameter value increases, $\mathbf{R}_s$ will also increase. Conversely, a negative sensitivity index indicates that $\mathbf{R}_s$ will decrease as the parameter value increases. The main factors that affect the probability of IVF success can be found using any of these techniques. The study suggests that increasing parameters $\alpha_1, \alpha_2, \alpha_3, \gamma_1, \gamma_2,$ and γ_3 increase $\mathbf{R}_s$, while increasing parameters μ, and σ, decrease it. Fig. 3 depicts simulation results for various parameter effects on $\mathbf{R}_s$, which are within a feasible domain, and it clarifies the effect of each parameter on the IVF success threshold.

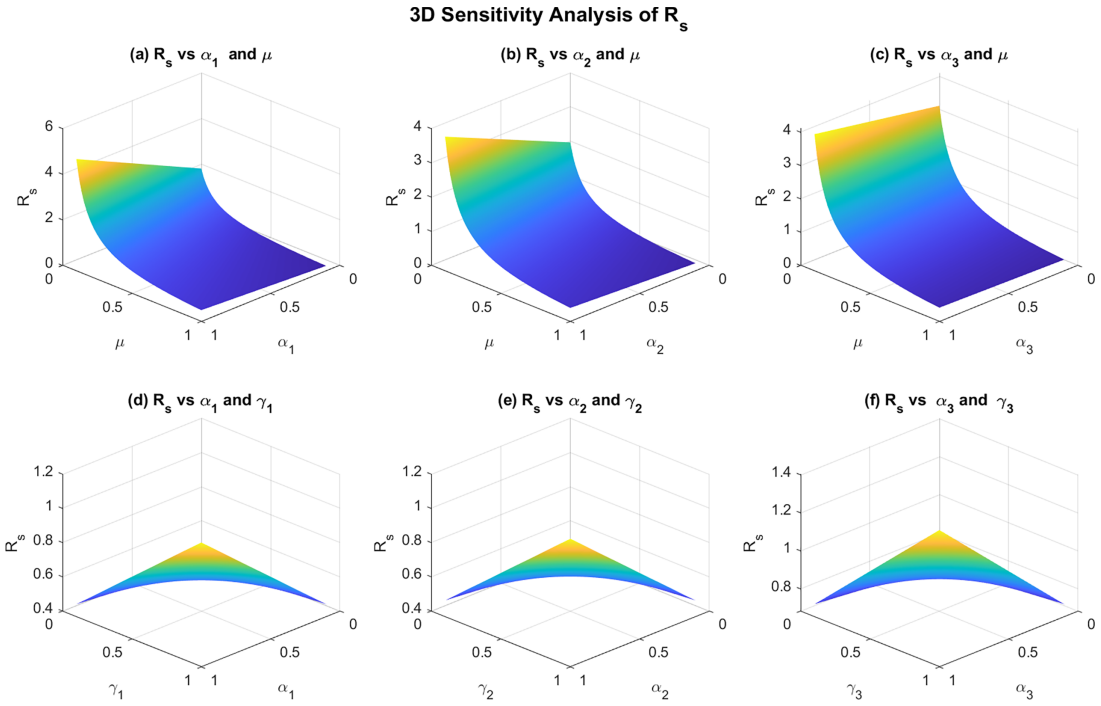

Figure 3: Analysis of R_s with different parameters.

4.4 Boundedness and Positivity of the System

This study looks at the conditions under which the proposed model, whose output is guaranteed to be bounded and positive, can be applied in real-world scenarios. The following are true $\forall t \geq 0$ as the classical derivatives:

$$
\begin{aligned}
&I(t) \geq I_0 e^{-(\mu_1+\beta)t},\\
&V(t) \geq V_0 e^{-(\mu_2+\alpha_1+\alpha_2+\alpha_3)t},\\
&G_1(t) \geq G_{1_0} e^{-(\gamma_1+\mu)t},\\
&G_2(t) \geq G_{2_0} e^{-(\gamma_2+\mu)t},\\
&G_3(t) \geq G_{3_0} e^{-(\gamma_3+\mu)t},\\
&F(t) \geq F_0 e^{-\mu t}.
\end{aligned} \tag{10}
$$

As long as the initial conditions of the Caputo fractional operator are met $\forall t > 0$, the system (5) solution will remain positive [29], resulting in:

$$I(t) \geq I_0 \, \mathfrak{e}_\tau\{-(\mu_1 + \beta)t^\tau\},$$

$$
\begin{aligned}
&V(t) \geq V_0\ \mathfrak{e}_\tau\{-(\alpha_3+\alpha_2+\alpha_1+\mu_2)t^\tau\},\\
&G_1(t) \geq G_{1_0}\ \mathfrak{e}_\tau\{-(\gamma_1+\mu)t^\tau\},\\
&G_2(t) \geq G_{2_0}\ \mathfrak{e}_\tau\{-(\gamma_2+\mu)t^\tau\},\\
&G_3(t) \geq G_{3_0}\ \mathfrak{e}_\tau\{-(\gamma_3+\mu)t^\tau\},\\
&F(t) \geq F_0\ \mathfrak{e}_\tau\{-(\mu)t^\tau\}.
\end{aligned} \tag{11}
$$

4.5 The Positively Invariant Region

Theorem 1: *The initial conditions that provided by the system's solutions of (5) in the positive region $\mathbb{R}^5_+$ are not negative.*

Proof: The positive outcomes of the model (5) are:

$$
\begin{aligned}
&{}^{C}D_t^\tau I(t)\big|_{I=0} = \pi N \geq 0,\\
&{}^{C}D_t^\tau V(t)\big|_{V=0} = \beta V \geq 0,\\
&{}^{C}D_t^\tau G_1(t)\big|_{G_1=0} = \alpha_1 V \geq 0,\\
&{}^{C}D_t^\tau G_2(t)\big|_{G_2=0} = \alpha_2 V \geq 0,\\
&{}^{C}D_t^\tau G_3(t)\big|_{G_3=0} = \alpha_3 V \geq 0,\\
&{}^{C}D_t^\tau F(t)\big|_{F=0} = (\gamma_1 G_1+\gamma_2 G_2+\gamma_3 G_3)\frac{1}{1+\sigma E} \geq 0.
\end{aligned} \tag{12}
$$

In consequence, we have

$$
\tilde{\prod} = (I, V, G_1, G_2, G_3, F) \in \mathbb{R}^6_+. \tag{13}
$$

The region $\tilde{\prod}$ is positively invariant. □

4.6 The Uniqueness and the Existence of the System

This section uses the fixed-point theorem to investigate the existence and uniqueness of the proposed model. While Schauder's fixed-point theorem ensures the model's existence, Banach's contraction theorem ensures the singularity of the model. If there is a solution, the appropriate approximation for it can be made using numerical approaches for $0 < \kappa \leq 1$. It is possible to make a system (5) more applicable by employing a fractional derivative in the Caputo sense. Let

$$
\begin{aligned}
&\lambda_1(t, I) = \pi N - \mu_1 I - \beta I,\\
&\lambda_2(t, V) = \beta I - (\mu_2+\alpha_1+\alpha_2+\alpha_3)V,\\
&\lambda_3(t, G_1) = \alpha_1 V - (\gamma_1+\mu)G_1,\\
&\lambda_4(t, G_2) = \alpha_2 V - (\gamma_2+\mu)G_2,\\
&\lambda_5(t, G_3) = \alpha_3 V - (\gamma_3+\mu)G_3,\\
&\lambda_6(t, F) = (\gamma_1 G_1+\gamma_2 G_2+\gamma_3 G_3)\frac{1}{1+\sigma E} - \mu F.
\end{aligned} \tag{14}
$$

Now, apply the fractional integral and initial conditions, to get;

$$
I(t) = I_0 + \frac{1}{\Gamma(\tau)}\int_0^t (t-\omega)^{\tau-1}\rho_1(t, I)d\omega,
$$

$$V(t) = V_0 + \frac{1}{\Gamma(\tau)} \int_0^t (t-\omega)^{\tau-1} \rho_2(t, V) d\omega,$$
$$G_1(t) = G_{1_0} + \frac{1}{\Gamma(\tau)} \int_0^t (t-\omega)^{\tau-1} \rho_3(t, G_1) d\omega,$$
$$G_2(t) = G_{2_0} + \frac{1}{\Gamma(\tau)} \int_0^t (t-\omega)^{\tau-1} \rho_4(t, G_2) d\omega,$$
$$G_3(t) = G_{3_0} + \frac{1}{\Gamma(\tau)} \int_0^t (t-\omega)^{\tau-1} \rho_5(t, G_3) d\omega,$$
$$F(t) = F_0 + \frac{1}{\Gamma(\tau)} \int_0^t (t-\omega)^{\tau-1} \rho_6(t, F) d\omega. \tag{15}$$

Let

$$\Lambda(t) = \begin{cases} I(t) \\ V(t) \\ G_1(t) \\ G_2(t) \\ G_3(t) \\ F(t) \end{cases}, \psi_0 = \begin{cases} I_0 \\ V_0 \\ G_{1_0} \\ G_{2_0} \\ G_{3_0} \\ F_0 \end{cases}, \aleph\mu, \Lambda(\mu) = \begin{cases} \lambda_1(t, I), \\ \lambda_2(t, V), \\ \lambda_3(t, G_1), \\ \lambda_4(t, G_2), \\ \lambda_5(t, G_3), \\ \lambda_6(t, F). \end{cases} \tag{16}$$

Therefore, the system (15) can be written as,

$$\varrho\,(t) = \varrho_0 + \frac{1}{\Gamma(\tau)} \int_0^t (t-\omega)^{\tau-1} \aleph(\omega), \varrho\,(\omega) d\omega. \tag{17}$$

The Banach space $\wp[0, \mathbb{Q}] = \varepsilon$ is found on a norm:

$$\|I, V, G_1, G_2, G_3, F\| = \max_{t \in [0, \mathbb{Q}]} [|I, V, G_1, G_2, G_3, F|]. \tag{18}$$

Define a mapping as $Y : \varepsilon \to \varepsilon$

$$Y\ \varrho\,(t) = \varrho_0 + \frac{1}{\Gamma(\tau)} \int_0^t (t-\omega)^{\tau-1} \aleph(\omega), \varrho\,(\omega) d\omega. \tag{19}$$

Using the assumptions given bellow on a non-linear function:

(P1) A constants $\eta_m, \eta_m > 0$ exists, so that

$$|\aleph(t, \varrho\,(t)| \leq \eta_m |\,\varrho\,(t)| + \eta_m. \tag{20}$$

(P2) A constant $\zeta_m > 0$ exists for each $\varrho, \bar{\varrho} \in \varepsilon$ such that

$$|\aleph(t, \bar{\varrho}) - \aleph(t, \bar{\varrho}_1)| \leq \zeta_m |\bar{\varrho} - \bar{\varrho}_1|. \tag{21}$$

Theorem 2: *Now, if* $(P1)$ *is true, then the system (5) will contain at least one solution.*

Proof: To show that Y is bounded, assume that $\phi = \{\varrho \in \phi | \eta \geq \| \varrho \|\}$, where η,

$$\eta \geq \max_{t\in[0,\mathbb{Q}]} \frac{\varrho_0 + \left(\frac{\eta_m \mathbb{Q}^\tau}{\Gamma(\tau+1)}\right)}{1 - \left(\frac{\eta_m \mathbb{Q}^\tau}{\Gamma(\tau+1)}\right)}, \tag{22}$$

is closed subset of ε.

$$\begin{aligned}
\| Y\ \varrho \| &= \max_{t\in[0,\mathbb{Q}]} | \varrho_0 + \frac{1}{\Gamma(\tau)} \int_0^t (t-\omega)^{\tau-1} \aleph(\omega, \varrho\ (\omega) d\omega| \\
&\leq | \varrho_0 | + \frac{1}{\Gamma(\tau)} \int_0^t (t-\omega)^{\tau-1} |\aleph(\omega, \varrho\ (\omega)| d\omega \\
&\leq | \varrho_0 | + \frac{1}{\Gamma(\tau)} \int_0^t (t-\omega)^{\tau-1} [\eta_m | \varrho\ (t)| + \eta_m] d\omega \\
&\leq | \varrho_0 | + [\eta_m \| \varrho \| + \eta_m] \frac{\mathbb{Q}^\tau}{\Gamma(\tau+1)} \leq \eta.
\end{aligned} \tag{23}$$

As $\varrho \in \phi \Rightarrow Y(\phi) \subseteq \phi$, it proves that Y is named to be bounded. Now, let $t_1 < t_2 \in [0, \mathbb{Q}]$, to prove that Y is continuous.

$$\begin{aligned}
\| Y\ \varrho\ (t_2) - Y\ \varrho\ (t_1) \| =& | \frac{1}{\Gamma(\tau)} \int_0^{t_2} (t_2-\omega)^{\tau-1} \aleph(\omega), \varrho\ (\omega) d\omega \\
&- \frac{1}{\Gamma(\tau)} \int_0^{t_1} (t_1-\omega)^{\tau-1} \aleph(\omega), \varrho\ (\omega) d\omega| \\
&\leq [\eta_m \| \varrho \| + \eta_m] \frac{[t_2^\tau - t_1^\tau]}{\Gamma(\tau+1)}.
\end{aligned} \tag{24}$$

This proves that $\| Y\ \varrho\ (t_2) - Y\ \varrho\ (t_1) \| \to 0$ as $t_2 \to t_1$, using Arzela- Ascoli theory, then the operator Y can be considered as continuous function. Thus, using Schauder's fixed point theory on the system (5) has at least one solution. Then, the system (5) has a unique solution that obtained by applying the Banach fixed point theorem. □

Theorem 3: *Let (5) gives a unique solution if the condition of* $(P2)$ *are hold.*

Proof: Let $\bar{\varrho}, \bar{\varrho}_1 \in \varepsilon$. Then

$$\begin{aligned}
\| Y(\bar{\varrho}) - Y(\bar{\varrho}_1) \| =& \max_{t\in[0,\mathbb{Q}]} | \frac{1}{\Gamma(\tau)} \int_0^t (t_2-\omega)^{\tau-1} \aleph(\omega, \bar{\varrho}(\omega) d\omega \\
&- \frac{1}{\Gamma(\tau)} \int_0^t (t_1-\omega)^{\tau-1} \aleph(\omega, \bar{\varrho}_1(\omega) d\omega| \\
&\leq \frac{Q^\tau}{\Gamma(\tau+1)} \zeta_m |\bar{\varrho} - \bar{\varrho}_1|.
\end{aligned} \tag{25}$$

Therefore Y can be considered as a contradiction. By using Banach fixed point theory, then the system (5) said to have a unique solution. □

Now, to show that the model actually satisfies the conditions mentioned before,

Consider the proposed IVF fractional order model written as:

$$D^\tau Y(t) = F(Y(t)), \quad 0 < \tau \leq 1,$$

where

$$Y(t) = (I, V, G_1, G_2, G_3, F)^T$$

where the function $F(Y) = AY$, with A being a constant matrix of biological transition rates.

Theorem 4: *Assume $F : \mathbb{R}^n \to \mathbb{R}^n$ be a continuous function satisfying the Lipschitz condition and linear growth condition. Then, the fractional differential system shows a unique solution on a given interval [25].*

Proof: To prove the conditions for the proposed model, the system can be classified to be linear with:

$$F(Y) = AY.$$

For any $Y, Z \in \mathbb{R}^6$, we have:

$$\|F(Y) - F(Z)\| = \|A(Y - Z)\|.$$

Using properties of matrix norms, it follows that:

$$\|F(Y) - F(Z)\| \leq \|A\|\|Y - Z\|,$$

which shows that F satisfies the Lipschitz condition with Lipschitz constant $L = \|A\|$.

Furthermore,

$$\|F(Y)\| = \|AY\| \leq \|A\|\|Y\|,$$

which Illustrates the linear growth condition.

Since both Lipschitz continuity and linear growth conditions are satisfied, The system provides a unique solution, according to classic results in fractional differential equations. □

5 Stability Analysis

Consider the fractional-order linear system:

$$D^\tau Y(t) = AY(t), \quad 0 < \tau \leq 1,$$

where

$$Y = (I, V, G_1, G_2, G_3, F)^T$$

illustrates the IVF compartments, and A is a constant matrix of biological transition rates.

Theorem 5 ([33]): *The equilibrium point $y^* = 0$ of the system is locally asymptotically stable if and only if all eigenvalues λ_i of the matrix A satisfy:*

$$|\arg(\lambda_i)| > \frac{\tau\pi}{2}, \quad \forall i.$$

In particular, if all eigenvalues satisfy:

$$\mathrm{Re}(\lambda_i) < 0,$$

then the system is locally asymptotically stable for any $0 < \tau \leq 1$.

$$\begin{bmatrix} -\mu_1 - \beta & 0 & 0 & 0 & 0 \\ \beta & -\mu_2 - \alpha_1 - \alpha_2 - \alpha_3 & 0 & 0 & 0 \\ 0 & \alpha_1 & -\gamma_1 - \mu & 0 & 0 \\ 0 & \alpha_2 & 0 & -\gamma_2 - \mu & 0 \\ 0 & \alpha_3 & 0 & 0 & -\gamma_3 - \mu. \end{bmatrix} \tag{26}$$

After checking the eigenvalues, which are determined using Maple software 2023, it was discovered that all of them were negative real values. Based on this, it can be said that the equilibrium point is locally stable.

The Lyapunov function can be used to determine the global stability of the equilibrium points, and the crucial lemma [34] can be used to examine the global stability of the suggested system.

Lemma 2: *For $t \geq t_0$, let $\mathrm{Q} \in \mathbb{R}^+$ be a continuous function. Then*

$$^{C}D_t^{\tau}\left(\mathrm{K} - \mathrm{D}^* - \mathrm{K}^* \log \frac{\mathrm{K}}{\mathrm{K}^*}\right) \leq \left(1 - \frac{\mathrm{K}^*}{\mathrm{K}}\right) {}^{C}D_t^{\tau}\mathrm{K}(t), \tag{27}$$

$\mathrm{K}^* \in \mathbb{R}^+ \forall \tau \in (0,1)$.

For the Lyapunov function, $\{I, V, G_1, G_2, G_3\}$, $L < 0$ is the equilibrium points $\mathbb{E}^*$.

Proof: Let the Volterra-type Lyapunov function:

$$\begin{aligned} L = {} & L_1\left(I - I^* - I^* \log \frac{I}{I^*}\right) + L_2\left(V - V^* - V^* \log \frac{V}{V^*}\right) \\ & + L_3\left(G_1 - G_1^* - G_1^* \log \frac{G_1}{G_1^*}\right) + L_4\left(G_2 - G_2^* - G_2^* \log \frac{G_2}{G_2^*}\right) \\ & + L_5\left(G_3 - G_3^* - G_3^* \log \frac{G_3}{G_3^*}\right) + L_6\left(F - F^* - F^* \log \frac{F}{F^*}\right), \end{aligned} \tag{28}$$

where L_i, $i = 1, 2, 3, 4$ are the positive constants. Then Lemma 2 can be used after substituting Eq. (28) into the system.

$$\begin{aligned} {}^{C}D_t^{\tau}L \leq {} & L_1\left(\frac{I - I^*}{I}\right) {}^{C}D_t^{\tau}I + L_2\left(\frac{V - V^*}{V}\right) {}^{C}D_t^{\tau}V + L_3\left(\frac{G_1 - G_1^*}{G_1}\right) {}^{C}D_t^{\tau}G_1 \\ & + L_4\left(\frac{G_2 - G_2^*}{G_2}\right) {}^{C}D_t^{\tau}G_2 + L_5\left(\frac{G_3 - G_3^*}{G_3}\right) {}^{C}D_t^{\tau}G_3 + L_6\left(\frac{F - F^*}{F}\right) {}^{C}D_t^{\tau}F. \end{aligned} \tag{29}$$

Now, substitute the derivative values in the above equation to have:

$$\begin{aligned} {}^{C}D_t^{\tau}L \leq {} & L_1\left(\frac{I - I^*}{I}\right)(\pi N - \mu_1 I - \beta I) + L_2\left(\frac{V - V^*}{V}\right)(\beta I - V(\mu_2 + \alpha_1 + \alpha_2 + \alpha_3)) \\ & + L_3\left(\frac{G_1 - G_1^*}{G_1}\right)(\alpha_1 V - G_1(\gamma_1 + \mu)) + L_4\left(\frac{G_2 - G_2^*}{G_2}\right)(\alpha_2 V - G_2(\gamma_2 + \mu)) \\ & + L_5\left(\frac{G_3 - G_3^*}{G_3}\right)(\alpha_3 V - G_3(\gamma_3 + \mu)) + L_6\left(\frac{F - F^*}{F}\right)((\gamma_1 G_1 + \gamma_2 G_2 + \gamma_3 G_3)\frac{1}{1 + \sigma E} - \mu F). \end{aligned} \tag{30}$$

Replacing $I = I - I^*$, $V = V - V^*$, $G_1 = G_1 - G_1^*$, $G_2 = G_2 - G_2^*$, $G_3 = G_3 - G_3^*$, $F = F - F^*$, to get;

$$^{C}D_t^{\tau}L \leq L_1\left(\frac{I - I^*}{I}\right)(\pi N - \mu_1(I - I^*) - \beta(I - I^*))$$

$$
\begin{aligned}
&+ L_2\left(\frac{V-V^*}{V}\right)(\beta(I-I^*)-(V-V^*)(\mu_2+\alpha_1+\alpha_2+\alpha_3))\\
&+ L_3\left(\frac{G_1-G_1^*}{G_1}\right)(\alpha_1(V-V^*)-(G_1-G_1^*)\gamma_1)\\
&+ L_4\left(\frac{G_2-G_2^*}{G_2}\right)(\alpha_2(V-V^*)-(G_2-G_2^*)\gamma_2)\\
&+ L_5\left(\frac{G_3-G_3^*}{G_3}\right)(\alpha_3(V-V^*)-(G_3-G_3^*)\gamma_3)\\
&+ L_6\left(\frac{F-F^*}{F}\right)(\gamma_1(G_1-G_1^*)+\gamma_2(G_2-G_2^*)+\gamma_3(G_3-G_3^*))\frac{1}{1+\sigma E}-\mu(F-F^*)).
\end{aligned}
\tag{31}
$$

Let $L_1 = L_2 = L_3 = L_4 = L_5 = 1$, then,

$$
\begin{aligned}
{}^{C}D_t^{\tau}L \le\ & (\pi N-\pi N\frac{I^*}{I}-\mu_1\frac{(I-I^*)^2}{I}-\beta\frac{(I-I^*)^2}{I})\\
&+(\beta I-\beta I^*-\beta I\frac{V^*}{V}+\beta I^*\frac{V^*}{V}-\frac{(V-V^*)^2}{V}(\mu_2+\alpha_1+\alpha_2+\alpha_3))\\
&+(\alpha_1 V-\alpha_1 V^*-\alpha_1 V\frac{G_1^*}{G_1}+\alpha_1 V^*\frac{G_1^*}{G_1}-\gamma_1\frac{(G_1-G_1^*)^2}{G_1})\\
&+(\alpha_2 V-\alpha_2 V^*-\alpha_2 V\frac{G_2^*}{G_2}+\alpha_2 V^*\frac{G_2^*}{G_2}-\gamma_2\frac{(G_2-G_2^*)^2}{G_2})\\
&+(\alpha_3 V-\alpha_3 V^*-\alpha_3 V\frac{G_3^*}{G_3}+\alpha_3 V^*\frac{G_3^*}{G_3}-\gamma_3\frac{(G_3-G_3^*)^2}{G_3})\\
&+\frac{\gamma_1 G_1}{1+\sigma E}-\frac{\gamma_1 G_1^*}{1+\sigma E}-\frac{\gamma_1 G_1 F^*}{(1+\sigma E)F}+\frac{\gamma_1 G_1^* F^*}{(1+\sigma E)F})\\
&+\frac{\gamma_2 G_2}{1+\sigma E}-\frac{\gamma_2 G_2^*}{1+\sigma E}-\frac{\gamma_2 G_2 F^*}{(1+\sigma E)F}+\frac{\gamma_2 G_2^* F^*}{(1+\sigma E)F})\\
&+\frac{\gamma_3 G_3}{1+\sigma E}-\frac{\gamma_3 G_3^*}{1+\sigma E}-\frac{\gamma_3 G_3 F^*}{(1+\sigma E)F}+\frac{\gamma_3 G_3^* F^*}{(1+\sigma E)F})-\mu\frac{(F-F^*)^2}{F}).
\end{aligned}
\tag{32}
$$

After simplification we get,

$$
{}^{C}D_t^{\tau}L \quad \le \quad \zeta_1-\zeta_2, \tag{33}
$$

where

$$
\begin{aligned}
\zeta_1 =\ & \pi N+\beta I+\beta I^*\frac{V^*}{V}+\alpha_1 V+\alpha_1 V^*\frac{G_1^*}{G_1}\\
&+\alpha_2 V+\alpha_2 V^*\frac{G_2^*}{G_2}+\alpha_3 V+\alpha_3 V^*\frac{G_3^*}{G_3}\\
&+\frac{\gamma_1 G_1}{1+\sigma E}+\frac{\gamma_1 G_1^* F^*}{(1+\sigma E)F}+\frac{\gamma_2 G_2}{1+\sigma E}+\frac{\gamma_2 G_2^* F^*}{(1+\sigma E)F}\\
&+\frac{\gamma_3 G_3}{1+\sigma E}+\frac{\gamma_3 G_3^* F^*}{(1+\sigma E)F},
\end{aligned}
$$

and.

$$\begin{aligned}\zeta_2 = {} & \pi N\frac{I^*}{I} + \mu_1\frac{(I-I^*)^2}{I} + \beta\frac{(I-I^*)^2}{I}) \\ & + \beta I^* + \beta I\frac{V^*}{V} + \frac{(V-V^*)^2}{V}(\mu_2+\alpha_1+\alpha_2+\alpha_3) + \alpha_1 V^* + \alpha_1 V\frac{G_1^*}{G_1} + \gamma_1\frac{(G_1-G_1^*)^2}{G_1} \\ & + \alpha_2 V^* + \alpha_2 V\frac{G_2^*}{G_2} + \gamma_2\frac{(G_2-G_2^*)^2}{G_2}) + \alpha_3 V^* + \alpha_3 V\frac{G_3^*}{G_3} + \gamma_3\frac{(G_3-G_3^*)^2}{G_3} \\ & + \frac{\gamma_1 G_1^*}{1+\sigma E} + \frac{\gamma_1 G_1 F^*}{(1+\sigma E)F} + \frac{\gamma_2 G_2^*}{1+\sigma E} + \frac{\gamma_2 G_2 F^*}{(1+\sigma E)F} \\ & + \frac{\gamma_3 G_3^*}{1+\sigma E} + \frac{\gamma_3 G_3 F^*}{(1+\sigma E)F} + \mu\frac{(F-F^*)^2}{F}.\end{aligned}$$

If

$$\zeta_1 < \zeta_2 \quad \Rightarrow \quad {}^{C}D_t^{\tau}L < 0.$$

But, if $I = I^*$, $V = V^*$, $G_1 = G_1^*$, $G_2 = G_2^*$, $G_3 = G_3^*$, $F = F^*$ then

$$\zeta_1 - \zeta_2 = 0, \quad \Rightarrow \quad {}^{C}D_t^{\tau}L = 0.$$

Therefore, we can conclude that if $\zeta_1 < \zeta_2$, the equilibrium points $\mathbb{E}^*$ are globally asymptotically stable in the invariant region. □

6 Numerical Algorithm for Computational Analysis

Caputo's derivative can be used to model power-law processes, as is well known from the literature. In order to incorporate power law effects into our model, we evaluated the dynamics seen in fractional calculus using the temporal derivative in conjunction with the Caputo derivative. A numerical method based on Newton polynomial interpolation can then be used to discretize the problem at hand [29,35]. One way to express the system (5) is:

$$\begin{aligned}
&{}^{C}D_t^{\tau}I(t) = \lambda_1(t,\Theta(t)),\\
&{}^{C}D_t^{\tau}V(t) = \lambda_2(t,\Theta(t)),\\
&{}^{C}D_t^{\tau}G_1(t) = \lambda_3(t,\Theta(t)),\\
&{}^{C}D_t^{\tau}G_2(t) = \lambda_4(t,\Theta(t)),\\
&{}^{C}D_t^{\tau}G_3(t) = \lambda_5(t,\Theta(t)),\\
&{}^{C}D_t^{\tau}F(t) = \lambda_6(t,\Theta(t)).
\end{aligned} \tag{34}$$

where $\Theta(t) = (I(t), V(t), G_1(t), G_2(t), G_3(t), F(t))$.

Let the general description of (34) be

$$\begin{cases} {}_0^{C}\mathrm{D}_t^{\tau}\mathrm{J}(t) = F(t,\mathrm{J}(t)), \quad \tau \in (0,1], \quad t \in [0,\mathbb{Q}], \\ \mathrm{J}(0) = \mathrm{J}_0. \end{cases} \tag{35}$$

Caputo Integral Representation

The Caputo derivative can be written as:

$$J(t) = J_0 + \frac{1}{\Gamma(\tau)} \int_0^t (t-\zeta)^{\tau-1} F(J(\zeta))\, d\zeta.$$

Time Discretization

Let the interval $[0, T]$ be divided into uniform steps:

$$t_\kappa = \kappa h, \quad \kappa = 0, 1, 2, \ldots, N,$$

where h is the step size.

Then:

$$J_{\kappa+1} = J_0 + \frac{1}{\Gamma(\tau)} \sum_{n=0}^{\kappa} \int_{t_n}^{t_{n+1}} (t_{\kappa+1}-\zeta)^{\tau-1} F(J(\zeta))\, d\zeta.$$

Newton Polynomial Interpolation

On each interval $[t_n, t_{n+1}]$, we approximate $F(j(\zeta))$ using the first-order Newton interpolation polynomial:

$$F(J(\zeta)) \approx F(J_n) + \frac{\zeta - t_n}{h} \left(F(J_{n+1}) - F(J_n)\right).$$

Substitution into the Integral

Substituting the interpolation into the integral yields:

$$\int_{t_n}^{t_{n+1}} (t_{\kappa+1}-\zeta)^{\tau-1} F(J(\zeta)) d\zeta = F(J_n) A_{\kappa,n} + F(J_{n+1}) B_{\kappa,n},$$

where the coefficients are given by:

$$A_{\kappa,n} = \int_{t_n}^{t_{n+1}} (t_{\kappa+1}-\zeta)^{\tau-1} \left(1 - \frac{\zeta - t_n}{h}\right) d\zeta,$$
$$B_{\kappa,n} = \int_{t_n}^{t_{n+1}} (t_{\kappa+1}-\zeta)^{\tau-1} \frac{\zeta - t_n}{h} d\zeta.$$

After simplification, these coefficients can be written as:

$$A_{\kappa,n} = \frac{h^\tau}{\Gamma(\tau+2)} \left[(\kappa+1-n)^{\tau+1} - (\kappa-n)^{\tau+1}\right],$$
$$B_{\kappa,n} = \frac{h^\tau}{\Gamma(\tau+2)} \left[(\kappa+1-n)^{\tau+1} - (\kappa-n)^{\tau+1} - \tau(\kappa-n)^\tau\right].$$

Final Discrete Scheme

Thus, the numerical solution is given by:

$$J_{\kappa+1} = J_0 + \frac{1}{\Gamma(\tau)} \sum_{n=0}^{\kappa} \left[A_{\kappa,n} F(J_n) + B_{\kappa,n} F(J_{n+1})\right].$$

Component-wise System

Applying this to the IVF compartments:

$$I_{\kappa+1} = I_0 + \frac{1}{\Gamma(\tau)} \sum_{n=0}^{\kappa} [A_{\kappa,n}(\pi N - \mu_1 I_n - \beta I_n) + B_{\kappa,n}(\pi N - \mu_1 I_{n+1} - \beta I_{n+1})]$$

$$V_{\kappa+1} = V_0 + \frac{1}{\Gamma(\tau)} \sum_{n=0}^{\kappa} \left[A_{\kappa,n}(\beta I_n - (\mu_2 + \alpha_1 + \alpha_2 + \alpha_3)V_n) + B_{n,j}(\beta I_{n+1} - (\mu_2 + \alpha_1 + \alpha_2 + \alpha_3)V_{j+1})\right]$$

$$G_{1,\kappa+1} = G_{1,0} + \frac{1}{\Gamma(\tau)} \sum_{n=0}^{\kappa} [A_{\kappa,n}(\alpha_1 V_n - (\mu + \gamma_1)G_{1,n}) + B_{\kappa,n}(\alpha_1 V_{n+1} - (\mu + \gamma_1)G_{1,n+1})]$$

$$G_{2,\kappa+1} = G_{2,0} + \frac{1}{\Gamma(\tau)} \sum_{n=0}^{\kappa} [A_{\kappa,n}(\alpha_2 V_n - (\mu + \gamma_2)G_{2,n}) + B_{\kappa,n}(\alpha_2 V_{n+1} - (\mu + \gamma_2)G_{2,n+1})]$$

$$G_{3,\kappa+1} = G_{3,0} + \frac{1}{\Gamma(\tau)} \sum_{n=0}^{\kappa} [A_{\kappa,n}(\alpha_3 V_n - (\mu + \gamma_3)G_{3,n}) + B_{\kappa,n}(\alpha_3 V_{n+1} - (\mu + \gamma_3)G_{3,n+1})]$$

$$F_{\kappa+1} = F_0 + \frac{1}{\Gamma(\tau)} \sum_{n=0}^{\kappa} \left[A_{\kappa,n}\left((\gamma_1 G_{1,n} + \gamma_2 G_{2,n} + \gamma_3 G_{3,n})\frac{1}{1+\sigma E}\right) - \mu F_j\right)\right]$$

$$+B_{n,j}\left(\frac{1}{1+\sigma E}(\gamma_1 G_{1,n+1} + \gamma_2 G_{2,n+1} + \gamma_3 G_{3,n+1}) - \mu F_{j+1}\right] \tag{36}$$

Fig. 4 shows the network-type flow chart for the solution algorithm in the proposed technique:

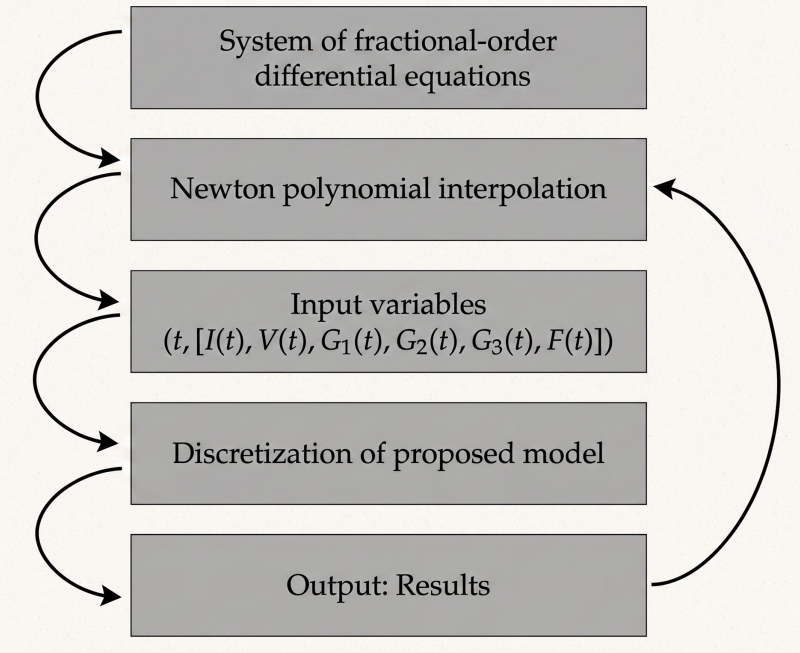

Figure 4: Solution algorithm.

6.1 Stability of Numerical Scheme

The initial value problem can be written as:

$${}_0^C D_t^{\tau} \psi(t) = \psi(t, \rho(t)), \quad \tau \in (0,1), \quad t \in [0, \mathrm{T}]. \tag{37}$$

Let ψ_{k+1} and $\overline{\psi}_{k+1}$ be numerical solutions to Eq. (37), with ψ_0 and $\overline{\psi}_0$ be the initial condition. If ϖ exists, such that

$$|\psi_{k+1} - \overline{\psi}_{k+1}| \leq \varpi_{\tau,\mathrm{T}} \|\psi_{k+1} - \overline{\psi}_{k+1}\|_\infty. \tag{38}$$

Thus, the model is stable will be the conclusion.

Lemma 3: *to get,*

$$\sum_{i=0}^{k+1} |p_i^{k+1}| \leq \varpi_\tau \mathrm{T}^\tau, \tag{39}$$

where ϖ_τ depends only on τ.

Theorem 6: *Let the solutions are denoted by* $\mathrm{y}_n(n = 1, 2, \ldots, k)$. *Then the suggested model is stable.*

Proof: Assume that ψ_0 and $\overline{\psi}_{k+1}$ be the initial conditions of Eq. (37), and let ψ_{k+1} and $\overline{\psi}_{k+1}$ be the numerical solutions to it. Now, let

$$|\psi_i - \overline{\psi}_n| \leq \varpi_{\tau,\mathrm{T}} \|\psi_0 - \overline{\psi}_0\|_\infty, \tag{40}$$

for $(n = 0, 1, 2, \ldots, k)$. It is is correct for $n = k + 1$. Keep in mind that the initial conditions are used to assume the induction basis $(n = 0)$.

$$\begin{aligned} |\psi_{k+1} - \overline{\psi}_{k+1}| \leq & \sum_{n=0}^{\lceil \tau \rceil - 1} \frac{t_{k+1}^n}{n!} |\psi_0^n - \overline{\psi}_0^n| + \frac{1}{\Gamma(\tau)} \Big[\sum_{n=0}^{k} |p_n^{k+1}| \left| f(t_n, \psi_n) - f(t_n, \overline{\psi}_n) \right| \\ & + |p_{k+1}^{k+1}| \left| f(t_{k+1}, \psi_{k+1}) - f(t_{k+1}, \overline{\psi}_{k+1}) \right| \Big] \\ \leq & \varpi_1 \|\psi_0 - \overline{\psi}_0\|_\infty + \frac{|\rho|}{\Gamma(\tau)} \Big[\sum_{n=0}^{k} |q_i^{k+1}| \, |\mathrm{X}_i - \overline{\mathrm{Y}}_i| + |p_{k+1}^{k+1}| \, |\psi_{k+1} - \overline{\psi}_{k+1}| \Big]. \end{aligned} \tag{41}$$

From Lemma 3, It was found that

$$\begin{aligned} |\psi_{k+1} - \overline{\psi}_{k+1}| & \leq \varpi_1 \|\psi_0 - \overline{\psi}_0\|_\infty + \frac{|\rho|}{\Gamma(\tau)} \Big[\varpi_{1,\tau} \mathrm{T}^\tau \max_{0 \leq n \leq k} |\chi_n - \overline{\chi}_n| + \varpi_{k+1,\tau} \mathrm{T}^\tau \, |\psi_{k+1} - \overline{\psi}_{k+1}| \Big] \\ & \leq \frac{1}{1 - \frac{(\rho | \varpi_{k+1,\tau} \mathrm{T}^\tau)}{\Gamma(\tau)}} \Big[\varpi_1 \|\psi_0 - \overline{\psi}_0\|_\infty + \frac{|\varrho|}{\Gamma(\eta)} + \varpi_{1,\tau} \max_{0 \leq n \leq k} \mathrm{T}^\tau \, |\psi_n - \overline{\psi}_n| \Big] \end{aligned} \tag{42}$$

A conclusion can be written for sufficiently small T by utilizing a mathematical induction and a sufficiently large constant $\varpi_{\tau,\mathrm{T}}$. □

6.2 Parameter Estimation

A data-driven optimization method was used to estimate the model parameters. Based on ranges documented in the literature, initial parameter values were chosen. To simulate realistic observations, synthetic clinical data were created. This process guarantees that the estimated parameters offer the best fit to the data. The mean squared error (MSE) between the observed data and the model output is minimized in order to formulate the parameter estimation problem as an optimization problem [36].

$$\mathrm{MSE}(\eta) = \frac{1}{n} \sum_{j=1}^{n} \left(F(t_j; \eta) - F_{\mathrm{data}}(t_j) \right)^2 \tag{43}$$

A comparison between the fitted model and the simulated data is presented in Fig. 5. The calibrated parameters effectively represent the underlying trend and dynamics of the system, as seen by the fitted curve closely matching the observed data points across the whole time frame. The consistency and lack of notable discrepancies between the model and the data attest to the efficacy of the estimating process.

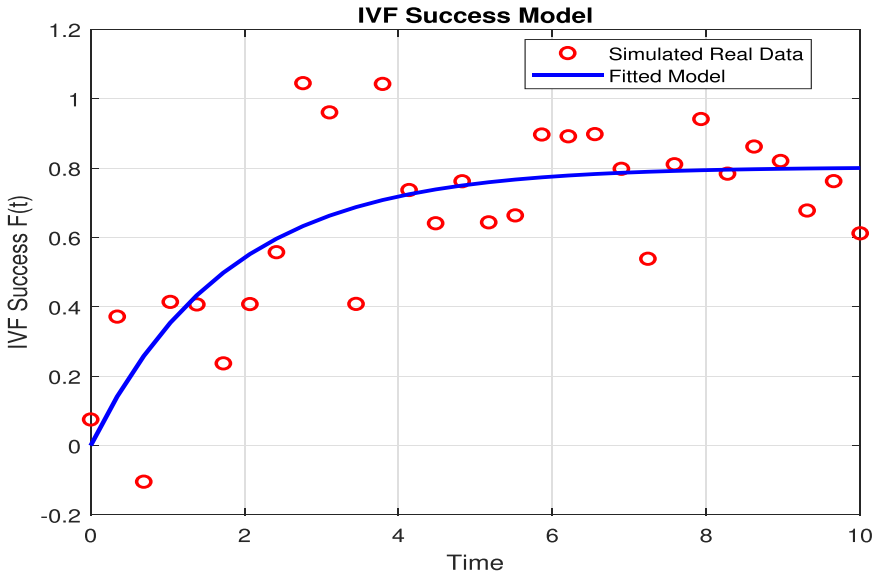

Figure 5: A comparison between the fitted model and the simulated data.

A common statistical metric used to quantify the discrepancies between values predicted by a model and those actually observed from the environment being modeled is the Root Mean Square Error (RMSE). It shows the square root of the second sample moment of the variations between the actual and expected values [37].

The$(RMSE)$ is calculated by:

$$RMSE = \sqrt{\frac{1}{n}\sum_{j=1}^{n}(q_j - \hat{q}_j)^2} \tag{44}$$

where:

- n is the number of data points;
- q_j is the actual values;
- $\hat{q}_j$ is the predicted values by the model.

The model fit's high accuracy is confirmed by the computed $(RMSE)$, which is minimal. The variation between the observed data and the model projections is known as the residual analysis [38], and it exhibits slight variations around zero with no discernible systematic pattern. This shows that there is no discernible bias and that the model accurately depicts the system's fundamental dynamics as shown in Fig. 6.

7 Results and Discussion

Data from the IVF clinic of Near East University Hospital database between 2015 and 2023 showed an overall increasing in the positive βHCG results except a little decline in 2019–2020 and the world wide

regulations and quarantine, then it was noticeable that the positive pregnancy is increasing till it reaches the maximum rate in 2022–2023 time interval, as illustrated in Table 3.

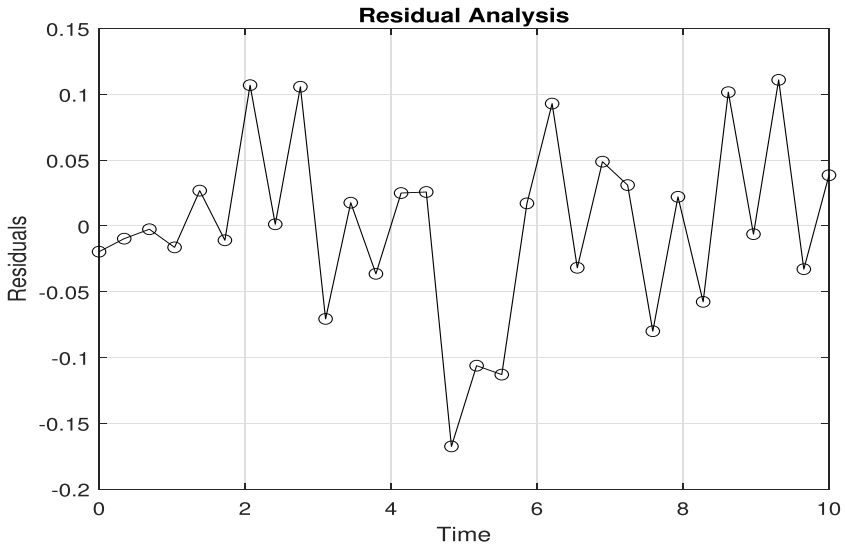

Figure 6: Residual analysis.

Table 3: Annual positive βHCG rates for IVF cycles from 2015 to 2023. [Near East University IVF clinic].

Year	Positive βHCG Percentage
2015–2016	20
2016–2017	32
2017–2018	43.4
2018–2019	54
2019–2020	44
2020–2021	55
2021–2022	60
2022–2023	78

Table 4 below, illustrates a comparison between a regular IVF program and Oocyte donation program positive outcomes, It was found that the rate of having positive βHCG is the highest when the recipient age is less than 35 in both programs and the rate of success of age over than 40 is higher 20 percent in oocyte donation program (all $p < 0.05, 95\% CI$).

Table 4: Recipient age vs. the success outcomes of regular IVF and Oocyte donation programs.

Age Groups of Recipients	Positive βHCG Rate for Regular IVF Program	Positive βHCG Rate for Oocyte Donation Program
Less than 35	0.46	0.70
35–40	0.41	0.68
Greater than 40	0.24	0.43

48.5 million couples globally suffer from infertility, with rates estimated to be between 3.5 and 16.7 percent in countries with moderate to low incomes [39]. According to European statistics, as many as one-quarter of patients who had their first IVF cycle quit their fertility treatment [40]. This is because of the treatment itself, which has side effects and is stressful, in addition to the expenses and negative outcome [41]. The main areas of satisfaction with fertility treatment include feeling satisfied with the centre, the number, length, and quality of treatments, as well as information about the type, negative effects, and outcome of each treatment [42]. As shown earlier in Table 1, significant factors were highlighted in the regular IVF program and the Donation program, such as using fresh embryos and implanting two or three embryos. Also, it was found that the recipient age is important in both regular IVF and donation programs, and the chance of pregnancy in older females increases in donation programs. The skill and expertise of the specialists aiding with *in vitro* fertilization continue to be vital. When it comes to specific groups of women, particularly older women who have historically had low success rates, it is now widely acknowledged that other factors are important in deciding the outcome. Furthermore, it is a common procedure to replace many embryos in an attempt to boost the possibility of pregnancy; however, this approach is becoming less and less sensible due to the high risk of multiple pregnancies [43]. Male or female factors in the integer-order model rapidly decline as the mechanism begins in the compartment of infertile couples diagnosed with Polycystic Ovary Syndrome (PCOS), indicating an immediate transition to therapy, according to the fractional model and the graphs below. The fractional-order model, which takes into consideration biological delays, treatment uncertainty, and time-dependent effects like recurrent consultations or lifestyle changes before IVF treatment, shows a steadier decline.

- The Fig. 7 shows a simulation of infertile couples with a PCOS diagnosis. The change in the I compartment when we switch to the fractional-order derivative order is depicted in Fig. 7a. The variation is shown in Fig. 7b by altering the fractional-order (τ). The diagnosis is made more quickly at a higher fractional order. It depicts different $I(t)$ levels for various τ values.

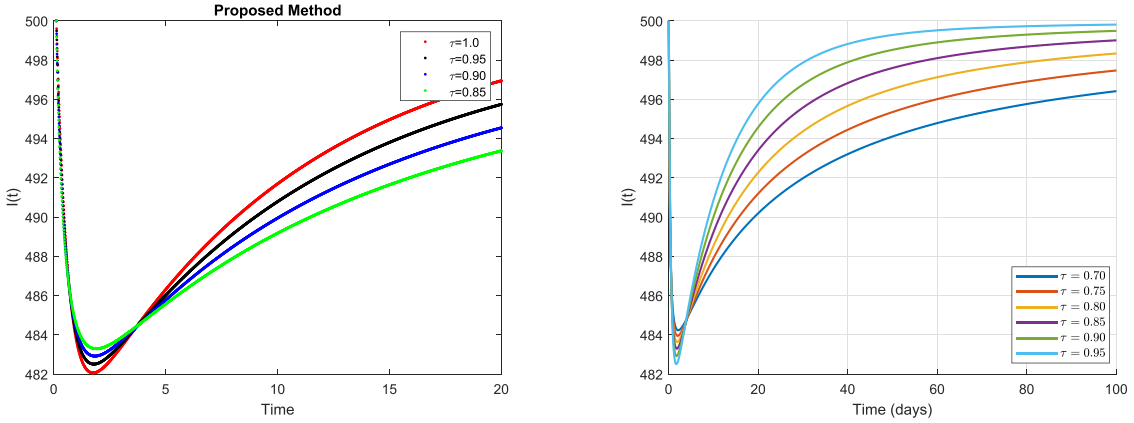

(**a**) Compare with Integer Order (**b**) Fractioanl Order dynamics

Figure 7: Simulation of $I(t)$ at various τ values with proposed operator.

- The number of patients undergoing IVF treatment, which includes ovarian stimulation, egg retrieval, sperm collection, and fertilization, is simulated in Fig. 8. Fig. 8a shows how the V compartment changes when we move to the fractional-order derivative order. Fig. 8b illustrates the variation by modifying the fractional-order (τ). At a higher fractional order, the IVF treatment is made faster. It illustrates the effects of varying τ values on the $V(t)$ population.

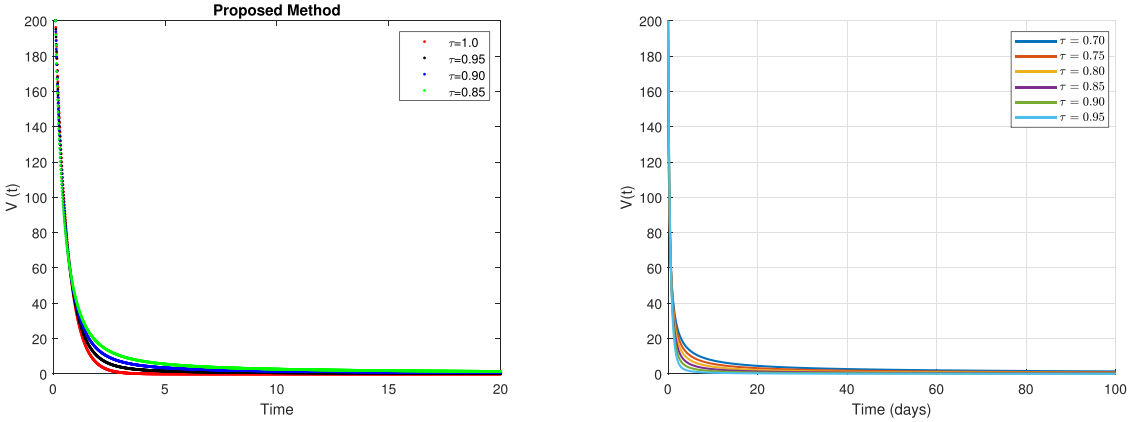

(**a**) Compare with Integer Order (**b**) Fractioanl Order dynamics

Figure 8: Simulation of $V(t)$ at various τ values with proposed operator.

- Fig. 9 illustrates a high-quality embryos' simulation. Fig. 9a shows how the fractional-order derivative order affects the G_1 compartment. Fig. 9b illustrates the variation caused by changing the fractional-order (τ). Higher fractional orders allow for a faster progression of high-quality embryos. It shows different $G_1(t)$ levels for various τ values. Lighter patches indicate higher values of $G_1(t)$, whereas darker patches indicate slower progress.

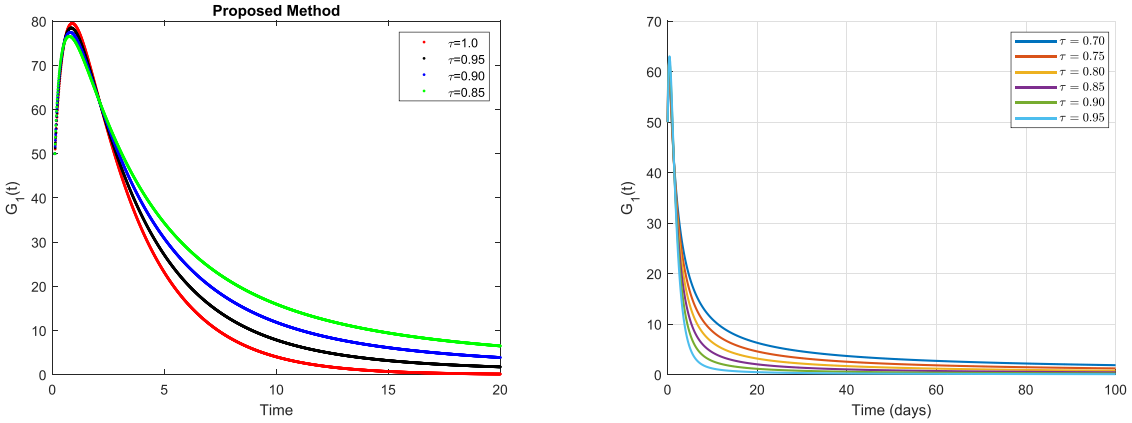

(**a**) Compare with Integer Order (**b**) Fractioanl Order dynamics

Figure 9: Simulation of $G_1(t)$ at various τ values with proposed operator.

- Fig. 10 depicts a simulation of embryos with medium quality. Fig. 10a shows how the G_2 compartment changes when we switch to the fractional-order derivative order. Fig. 10b depicts the variation when the fractional-order (τ) is altered. Higher fractional order allows for faster progression of medium-quality embryos. It displays different $G_2(t)$ levels for different τ values. Lighter patches show higher values of $G_2(t)$, whereas darker patches show slower progression.

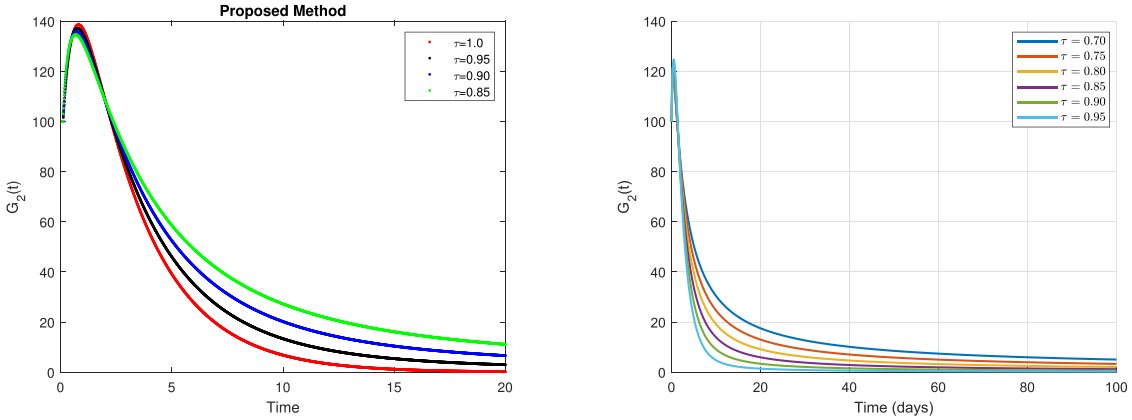

(**a**) Compare with Integer Order (**b**) Fractioanl Order dynamics

Figure 10: Simulation of $G_2(t)$ at various τ values with proposed operator.

- Low-quality embryos are simulated in the Fig. 11. Fig. 11a shows how the G_3 compartment changes when we move to the fractional-order derivative order. Fig. 11b illustrates the variation by modifying the fractional-order (τ). At a higher fractional order, the progression of low-quality embryos is noticed faster. For different τ values, it shows different $G_3(t)$ levels. Higher $G_3(t)$ values are indicated by lighter patches, whereas slower progression is indicated by darker patches.

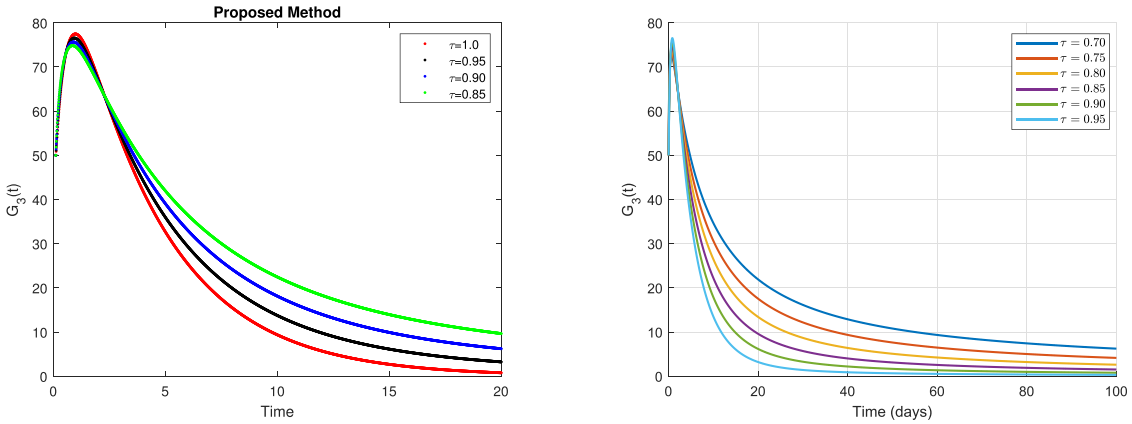

(**a**) Compare with Integer Order (**b**) Fractioanl Order dynamics

Figure 11: Simulation of $G_3(t)$ at various τ values with proposed operator.

- The Fig. 12 shows the number of positive pregnancy results. The effect of the fractional-order derivative order on the positive pregnancy instances is depicted in Fig. 12a. A variety of positive pregnancy cases resulting from altering the fractional-order (τ) are depicted in Fig. 12b. A quicker diagnosis is possible with higher fractional orders, which shows that the likelihood of a positive pregnancy rises as τ does.

The fractional order model for the patients undergoing IVF treatment, including ovarian stimulation, egg retrieval, sperm collection, and fertilization, shows a smoother and delayed transition, suggesting that certain patients require more time to participate completely in the treatment. For the embryo compartments, further gradual formation of embryos is achieved by the fractional order model, which also demonstrates a time-varying link in which responses from patient variation impact the rate of embryo development. The

fractional order model for the positive results of IVF shows a gradual but steady rise, which represents the long-term combined impact of several embryo transfers. This implies that fractional models better capture the progressive nature of IVF being successful, in which pregnancy may take several tries rather than happen all at once. Noted that the model parameters are adjusted to minimize the difference between predicted and observed IVF success outcomes using a least-squares approach.

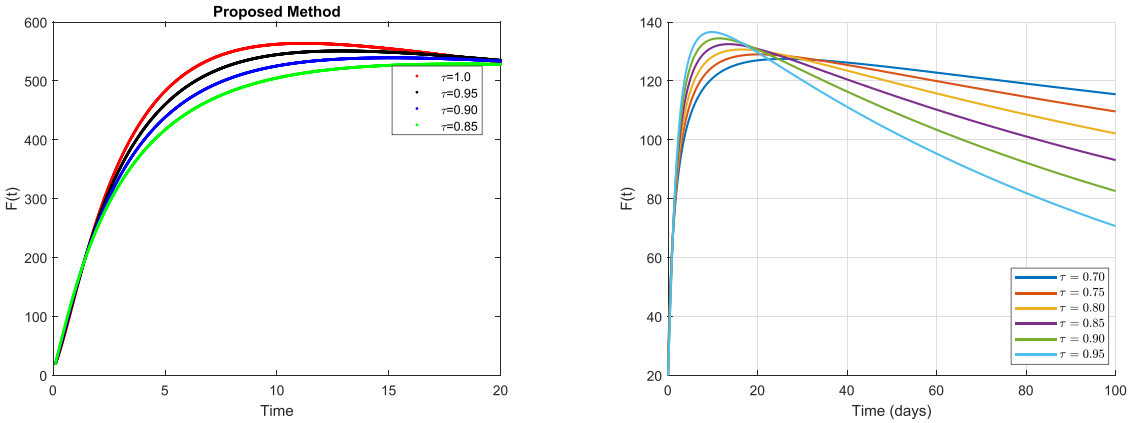

(**a**) Compare with Integer Order (**b**) Fractioanl Order dynamics

Figure 12: Simulation of $F(t)$ at various τ values with proposed operator.

Fractional derivatives take the system's history into consideration, in contrast to integer-order models (which are "memoryless"). Success in IVF depends on the cumulative physiological state, hormonal history, and prior interventions rather than just the present cycle. Fig. 13, illustrates this fact.

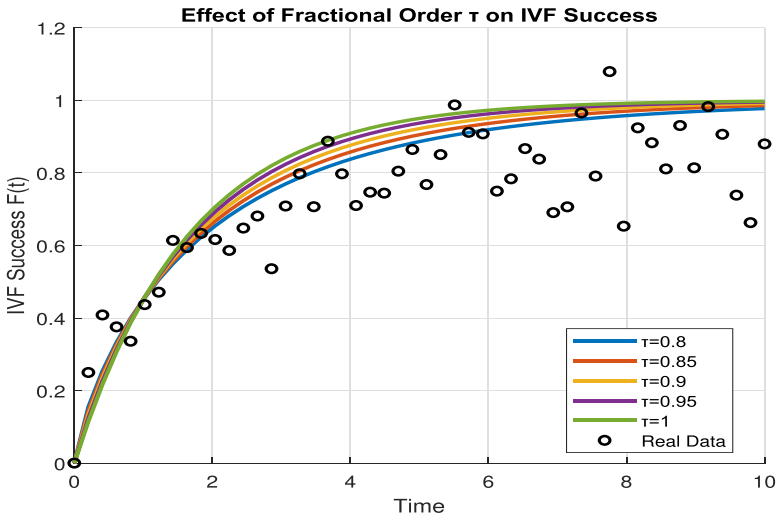

Figure 13: Effect of fractional order τ on IVF success.

The Root Mean Square Error $(RMSE)$ shows a strictly declining trend as τ is dropped from the classic example ($\tau = 1$), as seen in Table 5. In particular, compared to the integer-order model, the model at $\alpha = 0.80$ achieves an error reduction and offers a better localized fit to the clinical data points. This implies that non-local operators, which take into consideration the cumulative impacts of prior medical procedures, are a better representation of the underlying biological mechanisms of IVF.

Table 5: RMSE for different fractional orders (τ).

Fractional Order (τ)	RMSE Value
1.00 ($IntegerOrder$)	0.16
0.95	0.15
0.90	0.15
0.85	0.14
0.80	0.13

8 Conclusion

This study suggests the outcome of IVF treatment is significantly influenced by specific patient variables, particularly the age of the woman, as well as the experience of specific clinics. Moreover, it is evident that utilizing two or three embryos often results in improved overall IVF outcomes. Using the already accessible records, more research is required to determine whether IVF treatment is effective in certain situations. This suggests that infertile couples' decision-making is influenced by memory effects, which the integer order model may understate. The smoother response of the fractional model could more accurately reflect dropout rates and other slow physiological alterations, such as the effects of ovulation stimulation, that are not directly displayed by integer models. The slower development rate in the fractional model is consistent with real variations in ovarian response, embryonic growth phases, and implant opportunity delays. The study also examined the sensitivity of the reproductive number and established equilibrium points. The global stability of equilibrium points was validated by the Lyapunov function with integral inequality. Numerical simulations were used to illustrate the model's usefulness and show how it improved efficiency at different fractional orders. Our results confirm the significance of non-local Caputo derivatives in modeling for this, where the memory effect is crucial. The model of fractional order is more practical for determining ongoing IVF success because it more accurately reflects biological delays and memory effects in the real world. These results imply that fractional models need to be taken into account when arranging IVF treatments with the aim of more accurately reflecting the progressive process of therapy for infertility, as well as the results of gestation. Overall, the results demonstrate that the proposed modeling framework, when combined with the parameter estimate method, may effectively reproduce the observed behavior. This demonstrates the model's reliability and highlights how accurately it can depict the system's dynamics. The study analyzed data of 253 IVF patients collected from a single fertility clinic. While this data provides valuable insights for model development and validation, the relatively small sample size and single-center nature limit the generalizations of the findings to other populations or clinical settings. Selection bias may also be present, as patients attending this clinic may not represent the broader infertile population. Future studies with larger, multi-center datasets are necessary to validate and refine the proposed fractional-order model and to assess its predictive performance across diverse patient populations. In order to improve resource allocation tactics and get a deeper understanding of disease dynamics, further studies should investigate how the model can be applied under other differential operators and incorporate fractional derivatives using machine learning approaches for practical purposes.

Acknowledgement: The authors extend their appreciation to Prince Sattam bin Abdulaziz University for funding this research work through the project number (PSAU/2025/01/38405).

Funding Statement: The authors extend their appreciation to Prince Sattam bin Abdulaziz University for funding this research work through the project number (PSAU/2025/01/38405).

Author Contributions: Manal Ghannam: Conceptualization, Methodology, Investigation, Writing–Original Draft, Writing–Review and Editing, Visualization. Bilgen Kaymakamzade: Conceptualization, Methodology, Writing–Original Draft, Writing–Review and Editing, Software. Muhammad Farman: Methodology, Investigation, Writing–Review and Editing, Formal Analysis, Software. Kottakkaran Sooppy Nisar: Conceptualization, Methodology, Investigation, Software, Writing–Original Draft, Writing–Review and Editing, Visualization. Mohammed Altaf Ahmed: Formal Analysis, Investigation, Writing–Original Draft, Writing–Review and Editing, Visualization. All authors reviewed and approved the final version of the manuscript.

Availability of Data and Materials: The datasets analyzed during the current study are available from the corresponding author upon reasonable request.

Ethics Approval: The study was approved by the members of the Faculty of Medicine, Department of Medical Genetics, Near East University, Center of Excellent and Mathematics research center. All methods were carried out according to relevant guidelines and regulations. The ethical approval number is NEU/2024/121-1820. The data were anonymized and participant identities could not be identified so informed consent was not required.

Conflicts of Interest: The authors declare no conflicts of interest.

References

1. Vander Borght M, Wyns C. Fertility and infertility: definition and epidemiology. Clin Biochem. 2018;62(3):2–10. doi:10.1016/j.clinbiochem.2018.03.012.
2. Zegers-Hochschild F, Adamson GD, Mouzon J, Ishihara O, Mansour R, Nygren K, et al. International Committee for monitoring assisted reproductive technology (ICMART) and the world health organization (WHO) revised glossary of ART terminology. Fertil Steril. 2009;92(5):1520–4. doi:10.5935/1518-0557.2011.14.2.02.
3. Gleicher N, Kushnir VA, Barad DH. Worldwide decline of IVF birth rates and its probable causes. Hum Reprod Open. 2019;2019(3):hoz017. doi:10.1093/hropen/hoz017.
4. René C, Landry I, de Montigny F. Couples' experiences of pregnancy resulting from assisted reproductive technologies: a qualitative meta-synthesis. Int J Nurs Stud Adv. 2022;4(4):100059. doi:10.1016/j.ijnsa.2021.100059.
5. Van Loendersloot LL, van Wely M, Repping S, Bossuyt PMM, Van Der Veen F. Individualized decision-making in IVF: calculating the chances of pregnancy. Hum Reprod. 2013;28(11):2972–80. doi:10.1093/humrep/det315.
6. Steptoe PC, Edwards RG. Birth after the reimplantation of a human embryo. Lancet. 1978;312(8085):366. doi:10.1016/s0140-6736(78)92957-4.
7. Sharma V, Riddle A, Mason BA, Pampiglione J, Campbell S. An analysis of factors influencing the establishment of a clinical pregnancy in an ultrasound-based ambulatory *in vitro* fertilization program. Fertil Steril. 1988;49(3):468–78. doi:10.1016/s0015-0282(16)59775-1.
8. Sauer MV, Paulson RJ, Macaso TM, Francis MM, Lobo RA. Oocyte and pre-embryo donation to women with ovarian failure: an extended clinical trial. Fertil Steril. 1991;55(1):39–43. doi:10.1016/s0015-0282(16)54055-2.
9. Piette C, de Mouzon J, Bachelot A, Spira A. *In-vitro* fertilization: influence of women's age on pregnancy rates. Hum Reprod. 1990;5(1):56–9. doi:10.1093/oxfordjournals.humrep.a137041.
10. van Noord-Zaadstra BM, Looman CW, Alsbach H, Habbema JD, te Velde ER, Karbaat J. Delaying childbearing: effect of age on fecundity and outcome of pregnancy. BMJ. 1991;302(6789):1361–5. doi:10.1136/bmj.302.6789.1361.
11. Ubaldi FM, Cimadomo D, Vaiarelli A, Fabozzi G, Venturella R, Maggiulli R, et al. Advanced maternal age in IVF: still a challenge? the present and the future of its treatment. Front Endocrinol. 2019;10:94. doi:10.3389/fendo.2019.00094.
12. Johnson MH. A short history of *in vitro* fertilization (IVF). Int J Dev Biol. 2019;63(3–5):83–92. doi:10.1387/ijdb.180364mj.
13. Jansen RPS. Benefits and challenges brought by improved results from *in vitro* fertilization. Intern Med J. 2005;35(2):108–17. doi:10.1111/j.1445-5994.2004.00759.x.

14. de Ziegler D, Frydman R. Different implantation rates after transfers of cryopreserved embryos originating from donated oocytes or from regular *in vitro* fertilization. Fertil Steril. 1990;54(4):682–8. doi:10.1016/s0015-0282(16)53830-8.
15. Maehara K, Iwata H, Kimura K, Mori E. Experiences of transition to motherhood among pregnant women following assisted reproductive technology: a qualitative systematic review. JBI Evid Synth. 2022;20(3):725–60. doi:10.11124/jbies-20-00545.
16. Leushuis E, van der Steeg JW, Steures P, Bossuyt PMM, Eijkemans MJC, van der Veen F, et al. Prediction models in reproductive medicine: a critical appraisal. Hum Reprod Update. 2009;15(5):537–52. doi:10.1093/humupd/dmp013.
17. Sergeev S, Diakova I. Advanced KPI framework for IVF pregnancy prediction models in IVF protocols. Sci Rep. 2024;14(1):29477. doi:10.1038/s41598-024-80759-7.
18. Sarais V, Reschini M, Busnelli A, Biancardi R, Paffoni A, Somigliana E. Predicting the success of IVF: external validation of the van Loendersloot's model. Hum Reprod. 2016;31(6):1245–52. doi:10.1093/humrep/dew069.
19. Podlubny I. Fractional differential equations. San Diego, CA, USA: Academic Press; 1999.
20. Jajarmi A, Baleanu D, Arshad S, Wali M. Chapter 4—nonlinear fractional differential equation model analysis and application: a numerical approach and real data validation. In: Yavuz M, Singh DK, Townley S, editors. Recent developments in theory and applications of fractional order systems. San Francisco, CA, USA: Morgan Kaufmann; 2026. p. 51–65. doi:10.1016/B978-0-44-323952-6.00009-2.
21. Farman M, Nisar KS, Ali M, Ahmad H, Tabassum MF, Ghaffari AS. Chaos and forecasting financial risk dynamics with different stochastic economic factors by using fractional operator. Model Earth Syst Environ. 2025;11(2):146. doi:10.1007/s40808-025-02321-2.
22. Amilo D, Kaymakamzade B, Hincal E. A fractional-order mathematical model for lung cancer incorporating integrated therapeutic approaches. Sci Rep. 2023;13(1):12426. doi:10.1038/s41598-023-38814-2.
23. Almutairi N, Saber S, Ahmad H. The fractal-fractional Atangana-Baleanu operator for pneumonia disease: stability, statistical and numerical analyses. AIMS Math. 2023;8(12):29382–410. doi:10.3934/math.20231504.
24. Ng'oga MJ, Ndendya JZ. A Caputo fractional-order model for Foot-And-Mouth Disease with environmental transmission and intervention strategies. Microbe. 2026;10(4):100672. doi:10.1016/j.microb.2026.100672.
25. Podlubny I. Fractional differential equations: an introduction to fractional derivatives, fractional differential equations, to methods of their solution and some of their applications, vol. 198. Amsterdam, The Netherlands: Elsevier; 1998.
26. Richardson MC, Guo M, Fauser BCJM, Macklon NS. Environmental and developmental origins of ovarian reserve. Hum Reprod Update. 2014;20(3):353–69. doi:10.1093/humupd/dmt057.
27. INVITRA. General process of in vitro fertilization [Illustration]. In: INVITRA fertility treatments for couples. n.d. [cited 2026 May 17]. Available from: https://www.invitra.com/en/ivf-process/.
28. Mizuno S, Matsumoto H, Hashimoto S, Brahmajosyula M, Ohgaki A, Tarui S, et al. A novel embryo quality scoring system to compare groups of embryos at different developmental stages. J Assist Reprod Genet. 2021;38(5):1123–32. doi:10.1007/s10815-021-02117-0.
29. Ghannam M, Kaymakamzade B, Farman M, Nisar KS, Aljuaydi F, Sambas A. Investigating the success of Ivf with fractional-order model: analysis and case study. Fractals. 2026;34(02):2540255. doi:10.1142/s0218348x25402558.
30. Castillo-Garsow CW, Castillo-Chavez C. A tour of the basic reproductive number and the next generation of researchers. In: An introduction to undergraduate research in computational and mathematical biology: from birdsongs to viscosities. Cham, Switzerland: Springer; 2020. p. 87–124.
31. Magin RL. Fractional Calculus models of complex dynamics in biological tissues. Comput Math Appl. 2010;59(5):1586–93. doi:10.1016/j.camwa.2009.08.039.
32. Diekmann O, Heesterbeek JAP, Metz JAJ. On the definition and the computation of the basic reproduction ratio R0 in models for infectious diseases in heterogeneous populations. J Math Biol. 1990;28(4):365–82. doi:10.1007/bf00178324.
33. Matignon D. Stability results for fractional differential equations with applications to control processing. Comput Eng Syst Appl. 1996;2(1):963–8.

34. Bansal K, Mathur T, Agarwal S. Fractional-order crime propagation model with non-linear transmission rate. Chaos Solitons Fractals. 2023;169(12):113321. doi:10.1016/j.chaos.2023.113321.
35. Diethelm K. The analysis of fractional differential equations, Lecture notes in mathematics 2004. Berlin/Heidelberg, Germany: Springer; 2010.
36. Hastie T. The elements of statistical learning: data mining, inference, and prediction. New York, NY, USA: Springer; 2009.
37. Chai T, Draxler RR. Root mean square error (RMSE) or mean absolute error (MAE)?—Arguments against avoiding RMSE in the literature. Geosci Model Dev. 2014;7(3):1247–50. doi:10.5194/gmd-7-1247-2014.
38. Kutner MH, Nachtsheim CJ, Neter J, Li W. Applied linear statistical models. New York, NY, USA: McGraw, Irwin; 2005.
39. Chiware TM, Vermeulen N, Blondeel K, Farquharson R, Kiarie J, Lundin K, et al. IVF and other ART in low- and middle-income countries: a systematic landscape analysis. Hum Reprod Update. 2021;27(2):213–28. doi:10.1093/humupd/dmaa047.
40. Posaci C, Camus M, Osmanagaoglu K, Devroey P. Tubal surgery in the era of assisted reproductive technology: clinical options. Hum Reprod. 1999;14(Suppl 1):120–36. doi:10.1093/humrep/14.suppl_1.120.
41. Heijnen EMEW. What is the most relevant standard of success in assisted reproduction?: the next step to improving outcomes of IVF: consider the whole treatment. Hum Reprod. 2004;19(9):1936–8. doi:10.1093/humrep/deh368.
42. Hojgaard A, Ingerslev HJ, Dinesen J. Friendly IVF: patient opinions. Hum Reprod. 2001;16(7):1391–6. doi:10.1093/humrep/16.7.1391.
43. Templeton A. Assessing the outcome of IVF. Ann N Y Acad Sci. 2000;900(1):345–50. doi:10.1111/j.1749-6632.2000.tb06247.x.